

Odd and even magnetic resonant modes in highly overdoped $\text{Bi}_2\text{Sr}_2\text{CaCu}_2\text{O}_{8+\delta}$

L. Capogna^{1,2,3,*}, B. Fauqué⁴, Y. Sidis⁴, C. Ulrich³, P. Bourges⁴, S. Pailhès⁵,
A. Ivanov², J.L. Tallon⁶, B. Liang^{3,**}, C.T. Lin³, A.I. Rykov⁷, and B. Keimer³

¹ *INFM-CNR, 6 Rue J. Horowitz, 38042 Grenoble cedex 9, France*

² *Institut Laue-Langevin, 6 Rue J. Horowitz, 38042 Grenoble cedex 9, France*

³ *MPI für Festkörperforschung, Heisenbergstr. 1, 70569 Stuttgart, Germany*

⁴ *Laboratoire Léon Brillouin, CEA-CNRS, CEA-Saclay, 91191 Gif sur Yvette, France*

⁵ *LNS, ETH Zürich and Paul Scherrer Institute, 5232 Villigen PSI, Switzerland*

⁶ *Industrial Research Limited and Victoria University, P.O. 31310, Lower Hutt, New Zealand*

⁷ *Department of Applied Chemistry, University of Tokyo,
Hongo 7-3-1, Bunkyo-ku, Tokyo 113-8656, Japan*

We present inelastic neutron scattering data on highly overdoped $\text{Bi}_2\text{Sr}_2\text{CaCu}_2\text{O}_{8+\delta}$ single crystals with superconducting transition temperature $T_C = 70$ K and, for comparison, a nearly optimally doped crystal with $T_C = 87$ K. In both samples, magnetic resonant modes with odd and even symmetry under exchange of the two CuO_2 layers in the unit cell are observed. In the overdoped sample, the linewidth of the odd mode is reduced compared with the optimally doped sample. This finding is discussed in conjunction with recent evidence for intrinsic inhomogeneities in this compound. The data on odd and even resonant excitations are otherwise fully consistent with trends established on the basis of data on $\text{YBa}_2\text{Cu}_3\text{O}_{6+x}$. This confirms the universality of these findings and extends them into the highly overdoped regime of the phase diagram.

In high- T_C superconducting (SC) copper oxides, the experimental study of low-energy excitations is essential to building and testing microscopic models incorporating strong electronic correlations. Angle-resolved photoemission spectroscopy (ARPES) and inelastic neutron scattering (INS) are complementary momentum-resolved techniques to probe charge and spin excitation spectra, respectively. Comparison of ARPES and INS data is expected to shed light on the interaction between spin and charge excitations, which according to many models is at the root of the mechanism of high- T_C superconductivity¹. Among the different cuprate families, $\text{Bi}_2\text{Sr}_2\text{CaCu}_2\text{O}_{8+\delta}$ (Bi2212) is particularly suitable to carry out such a comparative study. Due to the high quality of its surface, this system has been widely investigated by ARPES². However, INS measurements were prohibited for a long time because of the small size of the single crystals.

This problem has recently been overcome thanks to the improvement in neutron flux on triple axis spectrometers, and to the use of arrays of co-aligned single crystals^{3,4,5}. ARPES studies have shown that in the underdoped and optimally doped regimes of the Bi2212 phase diagram, the system displays non-Fermi liquid properties with incoherent charge transport. The charge excitation spectrum displays pronounced anomalies around the $(\pi/a, 0)$ and $(0, \pi/a)$ wave vectors in the SC state: the so-called peak-dip-hump feature. At the same time, a spin-triplet excitation referred to as the magnetic resonant mode has been observed by INS in optimally doped³ and slightly overdoped⁴ Bi2212 at the planar wave vector $(\pi/a, \pi/a)$ approximately connecting the wave vectors at which the peak-dip-hump feature is observed in ARPES, and at a characteristic energy $E_r = 43$ meV that corresponds to the energy difference between the peak and the dip. As its counterpart in ARPES, this mode is only observed in the superconducting state. These observations point to a

strong scattering process involving spin-charge coupling.

Extensive INS studies of the magnetic resonant mode have been performed in $\text{YBa}_2\text{Cu}_3\text{O}_{6+x}$ (Y123)⁵, which shares its bilayer structure with Bi2212. In particular, it was shown that magnetic interactions between the two CuO_2 layers in a bilayer unit lead to the formation of two non-degenerate modes characterized by even and odd symmetries with respect to exchange of the layers^{6,7}. The relative spectral weight of the two modes allows incisive tests of microscopic models of the resonant mode as well as a determination of the bulk superconducting energy gap as a function of doping⁸. However, several drawbacks of the Y123 system make similar work on other families of high-temperature superconductors highly desirable. First, owing to problems with surface stability only limited ARPES data are available on this system^{9,10}, so that a quantitative comparison between ARPES and neutron scattering data has thus far not been carried out. Further, the Y123 crystal structure contains CuO chains, an electronically active but non-generic structural element. Although magnetic excitations originating from the CuO chains have thus far not been clearly identified, the influence of the chains on magnetic excitations in the CuO_2 planes is a matter of current debate^{11,12}. Finally, even with Ca substitution the doping levels accessible in Y123 are limited to the slightly overdoped regime.

Here we report the observation of even and odd magnetic excitations in the superconducting state of optimally doped and heavily overdoped Bi2212. The data encompass a doping level of $\delta = 0.21$ that has thus far only been reached in neutron scattering experiments on $\text{La}_{2-x}\text{Sr}_x\text{CuO}_4$ (Ref. 13). They are fully consistent with prior observations in Y123^{6,7,8} and unequivocally demonstrate the universal nature of the bilayer spin excitations, independent of materials-specific aspects of the crystal structure. They also greatly extend our capability to

correlate the results of INS and ARPES measurements in order to develop a quantitative description of the interaction between spin and charge excitations in the cuprates.

The INS measurements were performed, using the triple axis IN8 at the Institut Laue Langevin, Grenoble (France), on two $\text{Bi}_2\text{Sr}_2\text{CaCu}_2\text{O}_{8+\delta}$ single crystal specimens grown by the travelling solvent-floating zone method. The first one (OD87) was a monolithic, nearly optimally doped crystal of mass ~ 1.5 g and superconducting transition temperature $T_C = 87$ K. Though this sample is lightly overdoped, for convenience, we refer to it hereafter as optimally doped. The second sample (OD70) was an array of smaller crystals co-aligned using x-ray Laue diffraction on aluminium plates. Prior to alignment, the crystals were annealed at 420 °C under 7 bar of oxygen pressure for 5 days in order to increase the doping level well into the overdoped regime, so that T_C was reduced to 70 K. The quality of each crystal was assessed by inspecting the Laue diffraction pattern and the width of the superconducting transition (about 3 K) as determined by susceptibility measurements. The mosaic spread of the array was $\sim 1.6^\circ$, and its total mass was ~ 3 g. The INS experimental setup consisted of a pyrolytic graphite (PG) monochromator and a PG analyser, both set for the (002) reflection. No collimators were used in order to maximize the neutron flux. The samples were mounted in a He flow cryostat with the (H,H,0) and (0,0,L) crystal axes in the scattering plane. The wave vector transfer $\mathbf{Q} = (\text{H}, \text{K}, \text{L})$ is given in units of reciprocal lattice vectors $a^* \sim b^* = 1.64 \text{\AA}^{-1}$ and $c^* = 0.20 \text{\AA}^{-1}$. In most measurements the final neutron wave vector was fixed to $k_f = 4.1 \text{\AA}^{-1}$, and a PG-filter was inserted between the sample and the analyser to cut higher order contaminations. The energy resolution in this configuration is ~ 5 meV at the energy transfers studied. In order to extend the energy range, a configuration with $k_f = 5.5 \text{\AA}^{-1}$ (with no PG-filter and energy resolution ~ 8 meV) was also adopted, and intensity corrections were applied accordingly.

The dynamical spin susceptibility $\chi(\mathbf{Q}, \omega)$ of a bilayer system can be written as⁶

$$\chi(\mathbf{Q}, \omega) = \sin^2(\pi z L) \chi_o(\mathbf{Q}, \omega) + \cos^2(\pi z L) \chi_e(\mathbf{Q}, \omega)$$

where χ_o and χ_e denote components that are odd and even, respectively, under exchange of the layers. z denotes the layer separation expressed as a fraction of the unit cell dimension; $z = 0.108$ for Bi2212. The component of the momentum transfer perpendicular to the layers, L , can hence be used to select either odd or even components of χ .

In order to extract the magnetic contribution to the neutron scattering cross section, we followed procedures established in prior work on Y123 and Bi2212^{3,4,5}. In particular, it was shown that the magnetic resonant mode is sharply defined only in the superconducting state. The mode can thus be experimentally identified as a sharp enhancement in the difference of the neutron scattering

intensity between a low temperature (5K) and a temperature just above the superconducting transition temperature. Figures 1 and 2 show const- \mathbf{Q} scans at the in-plane wave vector transfer $\mathbf{Q}_{\parallel} = (0.5, 0.5)$, where the spectral weight of the magnetic resonant mode is known to be maximum. The out-of-plane component of the wave vector transfer was adjusted such that only odd excitations contribute to the signal. Both data sets indeed reveal the characteristic low-temperature enhancement of the cross section associated with the magnetic resonant mode^{3,4,5}. In order to ascertain the magnetic origin of the difference signal, the scans were repeated at $\mathbf{Q}_{\parallel} = (1.5, 1.5)$, keeping L fixed. At this position, a substantial reduction of the signal was observed. As phononic signals generally increase in higher Brillouin zones, this indicates that the signal is of magnetic origin. In both samples, the observed signals also exhibit other characteristic signatures of the magnetic resonant mode. Notably, the intensity enhancement is maximum around $\mathbf{Q}_{\parallel} = (0.5, 0.5)$ (not shown), and the intensity is gradually reduced upon heating and vanishes in an order-parameter-like fashion at the superconducting transition temperature (Fig. 3).

A comparison between the magnetic resonant modes in the odd channel of optimally doped and highly overdoped Bi2212 reveals interesting information. First, the mode energy decreases with doping. The energy of the mode in OD87, $E_r^o = 42$ meV, is consistent with prior work on optimally doped Bi2212. In the highly overdoped sample $E_r^o = 34$ meV, substantially lower than that determined in a previously studied, slightly overdoped sample /citehe, but consistent with the relationship $E_r^o = 5.4 k_B T_C$ established on the basis of extensive work on Y123 and Bi2212⁵. The new data therefore underscore our conclusion that this relation holds generally in the cuprates, and extend its range of validity into the highly overdoped regime.

Another interesting observation concerns the energy width of the resonant mode. In the optimally doped sample, the energy width of the resonant mode is much broader than the instrumental resolution. This agrees with prior work on optimally doped and slightly overdoped samples^{3,4}. Due to the high quality of our samples, combined with the fact that samples from different origins exhibit the same broadening, $\Delta_\omega \sim 11$ meV after a deconvolution of the energy resolution, it is unlikely that this broadening is of extraneous origin (arising, for instance, from a macroscopic oxygen concentration gradient). Remarkably, the odd peak in the overdoped sample is sharper, yielding $\Delta_\omega \sim 6$ meV after the resolution deconvolution. This observation mirrors the doping dependence of the inhomogeneity of the superconducting energy gap extracted from scanning tunnelling spectroscopy data on Bi2212¹⁴. This inhomogeneity arises from nanometer-sized patches with different SC gap magnitudes, which follow the distribution of oxygen dopant ions. In the overdoped range, the distribution of gap amplitudes is significantly reduced¹⁵. The parallel evolution of the width of (bulk-sensitive) neutron data on

the magnetic resonant mode suggests that the SC gap distribution is not a pure surface phenomenon. In Y123, however, the resonant mode is resolution-limited even at optimum doping⁵. The inhomogeneity is thus not generic to the cuprates, and it is not a precondition for high-temperature superconductivity.

We now turn to the measurements in the even channel, which is probed for $L = n/z$ with n integer (Figs. 1b and 2b). At optimum doping, the signal at this position (determined in the same way as the odd signal discussed above) exhibits an enhancement in the superconducting state centered at an energy transfer of $E_r^e = 54$ meV. Within the experimental error, this is identical to the energy of the even resonant mode recently identified in optimally doped Y123⁷. In the highly overdoped sample, a similar superconductivity-induced enhancement is observed around $E_r^e = 35$ meV. As in Y123, the even mode exhibits the same characteristics as the odd mode, including the temperature dependence of the intensity with its onset at T_C (Fig. 3). The even-odd splitting is thus dramatically reduced in the highly overdoped regime. This confirms and extends the trend established on the basis of data on overdoped Y123^{6,8}. In the overdoped sample, the even mode exhibits a larger energy linewidth compared with its odd counterpart. This feature is actually also observed in Y123 at all doping^{6,7,8}. The similarity of data on two distinct families of cuprates allows us to rule out materials-specific disorder as the origin of this broadening, so that an intrinsic mechanism appears to be at work.

As also observed in Y123^{6,7,8}, the intensity ratio of both modes intensities changes significantly with doping. More quantitatively, we have extracted the energy-integrated spectral weights of odd and even modes, $W_r^{o,e}$ ⁸. Using the fits of Fig. 1 and Fig. 2 and taking into account the fact that the scattering intensity

is further weighted by the magnetic form factor (which is L -dependent⁶), one deduces a ratio W_r^o/W_r^e varying from ~ 2.8 in OD87 to ~ 1.5 in OD70. As discussed in Refs. 8,16, an estimate of the threshold for particle-hole excitations in the superconducting state, ω_c , can then be obtained in the framework of the spin exciton model, where the spectral weight is approximately proportional to the binding energy of the resonant mode: $W_r^{o,e} \propto (\omega_c - E_r^{o,e})/\omega_c$. Fig. 4 provides a synopsis of the continuum threshold extracted in this way on the Bi2212 samples investigated here, along with analogous data on Y123. It is gratifying to see that the data on both systems are consistent. They are also consistent with the maximum superconducting energy gap extracted from ARPES¹⁷ and electronic Raman scattering (ERS)¹⁸ data also shown in Fig. 4. This finding is important, because neutron scattering is a bulk probe, while ARPES and ERS are sensitive to surface preparation. It also provides further reassurance of the validity of the spin exciton model.

In conclusion, our experiments have shown that the magnetic excitations in Y123 and Bi2212 evolve in a strikingly similar way, despite the different crystal structures and the presence of the electronically active CuO chains in Y123. This represents a significant step in the quest for a generic spin response of the cuprates. We were also able to establish parallels between the doping evolution of the width of the magnetic resonant mode and the gap disorder recently observed by scanning tunnelling spectroscopy on Bi2212 surfaces, indicating that at least part of this effect may be also representative of the bulk of Bi2212.

This work was supported in part by the Deutsche Forschungsgemeinschaft, Grant No. KE923/12 in the consortium FOR538.

* To whom correspondence should be addressed; E-mail: capogna@ill.fr

** Present address: Center for Superconductivity Research, Department of Physics, University of Maryland, College Park, Maryland 20742, USA.

¹ For a review, see M. Eschrig, *Adv. Phys.* **55**, 47 (2006).

² For a review, see J. C. Campuzano, M. R. Norman, and M. Randeria in "Physics of Conventional and Unconventional Superconductors", Vol. II, ed. K. H. Bennemann and J. B. Ketterson (Springer, Berlin, 2004), p. 167-273 (cond-mat/0209476).

³ H.F. Fong, P. Bourges, Y. Sidis, L.P. Regnault, A. Ivanov, G.D. Gu, N. Koshizuka, and B. Keimer, *Nature* **398**, 588 (1999).

⁴ H. He, Y. Sidis, P. Bourges, G.D. Gu, A. Ivanov, N. Koshizuka, B. Liang, C.T. Lin, L. P. Regnault, E. Schoenher, and B. Keimer, *Phys. Rev. Lett.* **86**, 1610 (2001).

⁵ For a review, see Y. Sidis, S. Pailhès, B. Keimer, P. Bourges, C. Ulrich, and L. Regnault, *Phys. Stat. Sol.* (b)

241, 1204 (2004).

⁶ S. Pailhès, Y. Sidis, P. Bourges, C. Ulrich, V. Hinkov, L.P. Regnault, A. Ivanov, C. Bernhard, B. Liang, C.T. Lin, and B. Keimer, *Phys. Rev. Lett.* **91**, 237002 (2003).

⁷ S. Pailhès, Y. Sidis, P. Bourges, V. Hinkov, A. Ivanov, C. Ulrich, L. P. Regnault, and B. Keimer *Phys. Rev. Lett.* **93**, 167001 (2004).

⁸ S. Pailhès, C. Ulrich, B. Fauqué, V. Hinkov, Y. Sidis, A. Ivanov, C.T. Lin, B. Keimer, and P. Bourges, *Phys. Rev. Lett.* **96**, 257001 (2006).

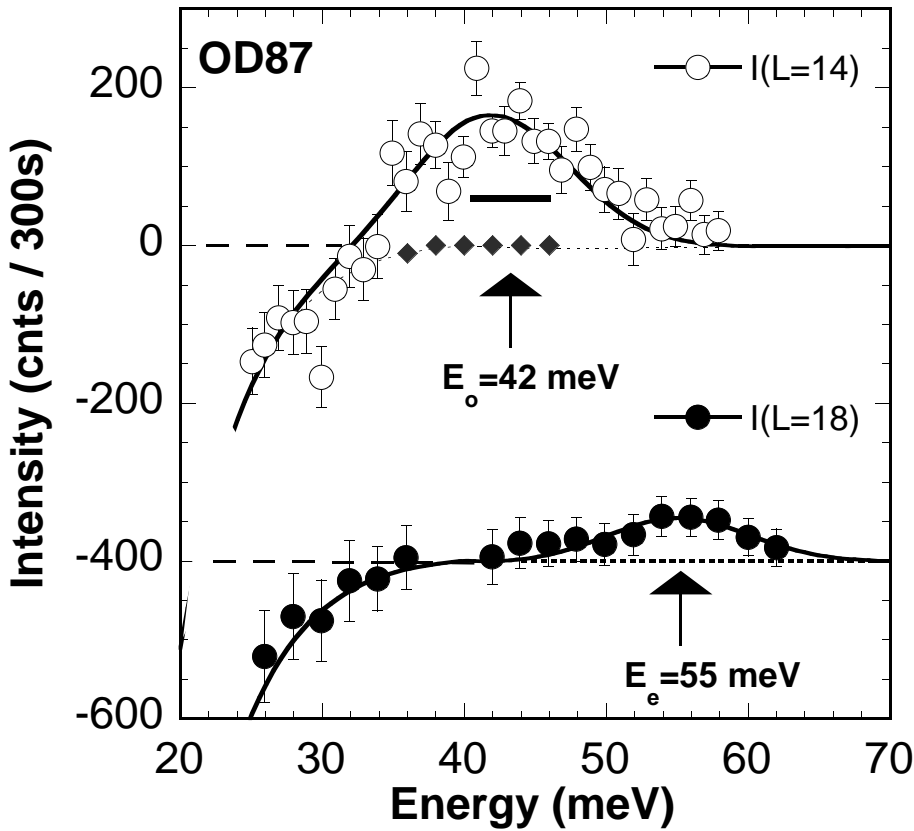
⁹ D. H. Lu, D. L. Feng, N. P. Armitage, K. M. Shen, A. Damascelli, C. Kim, F. Ronning, Z.-X. Shen, D. A. Bonn, R. Liang, W. N. Hardy, A. I. Rykov, and S. Tajima, *Phys. Rev. Lett.* **86**, 4370 (2001).

¹⁰ S. V. Borisenko, A. A. Kordyuk, V. Zabolotnyy, J. Geck, D. Inosov, A. Koitzsch, J. Fink, M. Knupfer, B. Büchner, V. Hinkov, C. T. Lin, B. Keimer, T. Wolf, S. G. Chiuazbian, L. Patthey, and R. Follath, *Phys. Rev. Lett.* **96**, 117004 (2006).

¹¹ H. Yamase and W. Metzner, *Phys. Rev. B* **73**, 214517

- (2006).
- ¹² I. Eremin and D. Manske, Phys. Rev. Lett. **94**, 067006 (2005).
 - ¹³ S. Wakimoto, H. Zhang, K. Yamada, I. Swainson, H. Kim, and R.J. Birgeneau, Phys. Rev. Lett. **92**, 217004 (2004).
 - ¹⁴ K. McElroy, J. Lee, J.A. Slezak, D.H. Lee, H. Eisaki, S. Uchida, J.C. Davis, Science **309**, 1048 (2005).
 - ¹⁵ J. Lee, K. Fujita, K. McElroy, J. A. Slezak, M. Wang, Y. Aiura, H. Bando, M. Ishikado, T. Masui, J.-X. Zhu, A. V. Balatsky, H. Eisaki, S. Uchida, and J. C. Davis, Nature **442** 546 (2006).
 - ¹⁶ A.J. Millis and H. Monien, Phys. Rev. B **54**, 16172 (1996).
 - ¹⁷ J. Mesot, M. Norman, H. Ding, M. Randeria, J. Cam-puzano, A. Paramekanti, H. Fretwell, A. Kaminski, T. Takeuchi, T. Yokoya, T. Sato, T. Takahashi, T. Mochiku, and K. Kadowaki, Phys. Rev. Lett. **83**, 840 (1999).
 - ¹⁸ See a compilation of ERS data in A. V. Chubukov, T. P. Devereaux, M. V. Klein, Phys. Rev. B **73**, 094512 (2006).

FIG. 1: Resonant magnetic modes in nearly optimally doped $\text{Bi}_2\text{Sr}_2\text{CaCu}_2\text{O}_{8+\delta}$ ($T_C=87$ K) (OD87) measured at $\mathbf{Q} = (0.5, 0.5, L)$ in the (a) odd channel ($L=14$) and (b) even channel ($L=18$). The signal is obtained by subtracting the intensity at $T=5\text{K}$ from the intensity above T_C . The full lines are the result of a fit by a Gaussian profile on top of a background (dotted lines). The shape of this background is given by the difference between the phonon populations at the two temperatures, yielding negative values at low energy. The diamond symbols correspond to the background level obtained by constant energy scans. Mn stands for monitor.



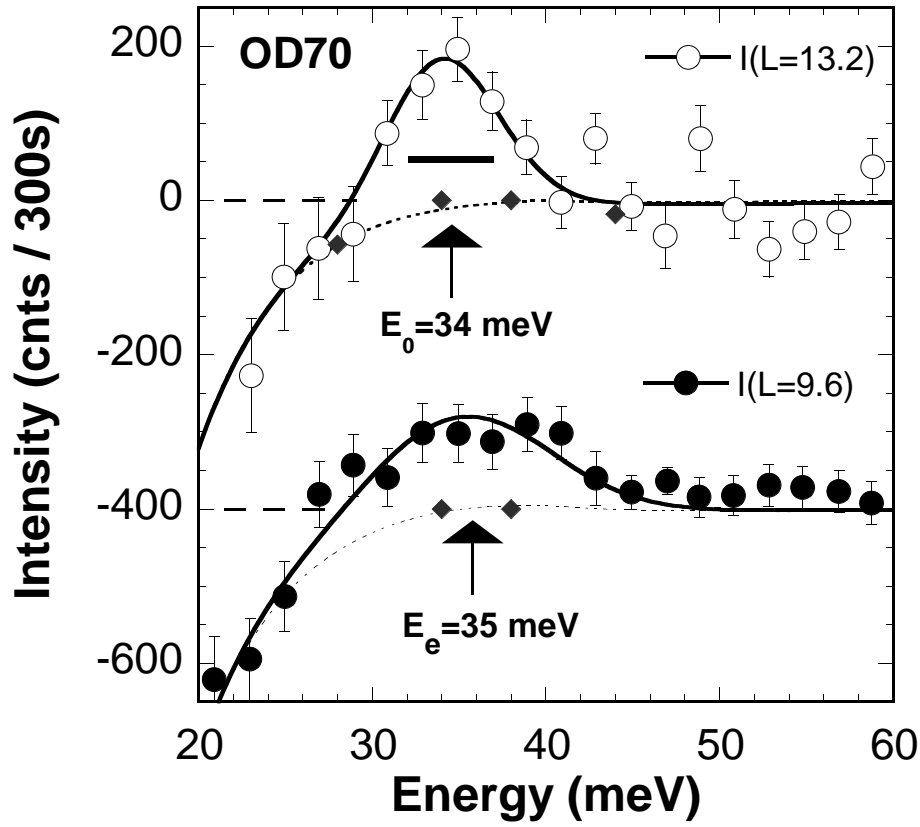


FIG. 2: Same as Fig. 1 in OD70, highly overdoped $\text{Bi}_2\text{Sr}_2\text{CaCu}_2\text{O}_{8+\delta}$ ($T_C=70$ K), in (a) odd channel ($L=13.2$) and (b) even channel ($L=9.6$). Note that the magnitude of the odd mode in absolute units is actually ~ 3 times weaker in OD70 than in OD87. An accurate value cannot be given due to uncertainties in the calibration procedure.

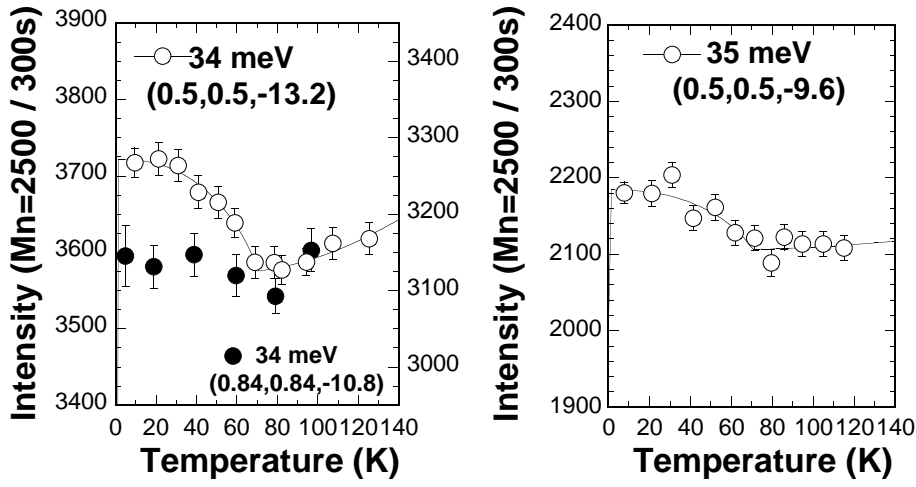


FIG. 3: Temperature dependence of the peak intensity of both odd (left panel) and even (right panel) resonant modes (empty symbols) in OD70. The solid symbols show the temperature evolution of the intensity at a background point away from the magnetic wave vector. The solid lines are the results of fits to the data obtained using a power law in the superconducting state on top of a phononic background.

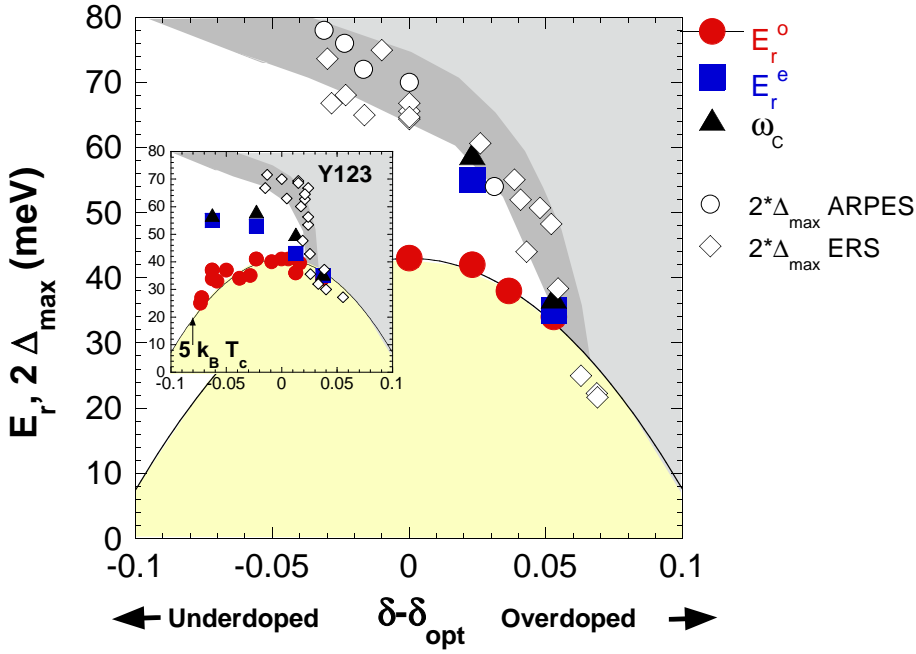


FIG. 4: Evolution of the magnetic resonant mode energy as a function of the hole concentration δ in the Bi2212 system. (see Ref. 8 for the definition of δ). The full symbols represent the odd (E_r^o) and even (E_r^e) modes, and the threshold energy (ω_c) as explained in the legend. The open symbols are the energy gap measured by ARPES¹⁷ and by Electronic Raman Scattering (ERS)¹⁸. The inset shows the equivalent diagram for Y123⁸.